DR2003103

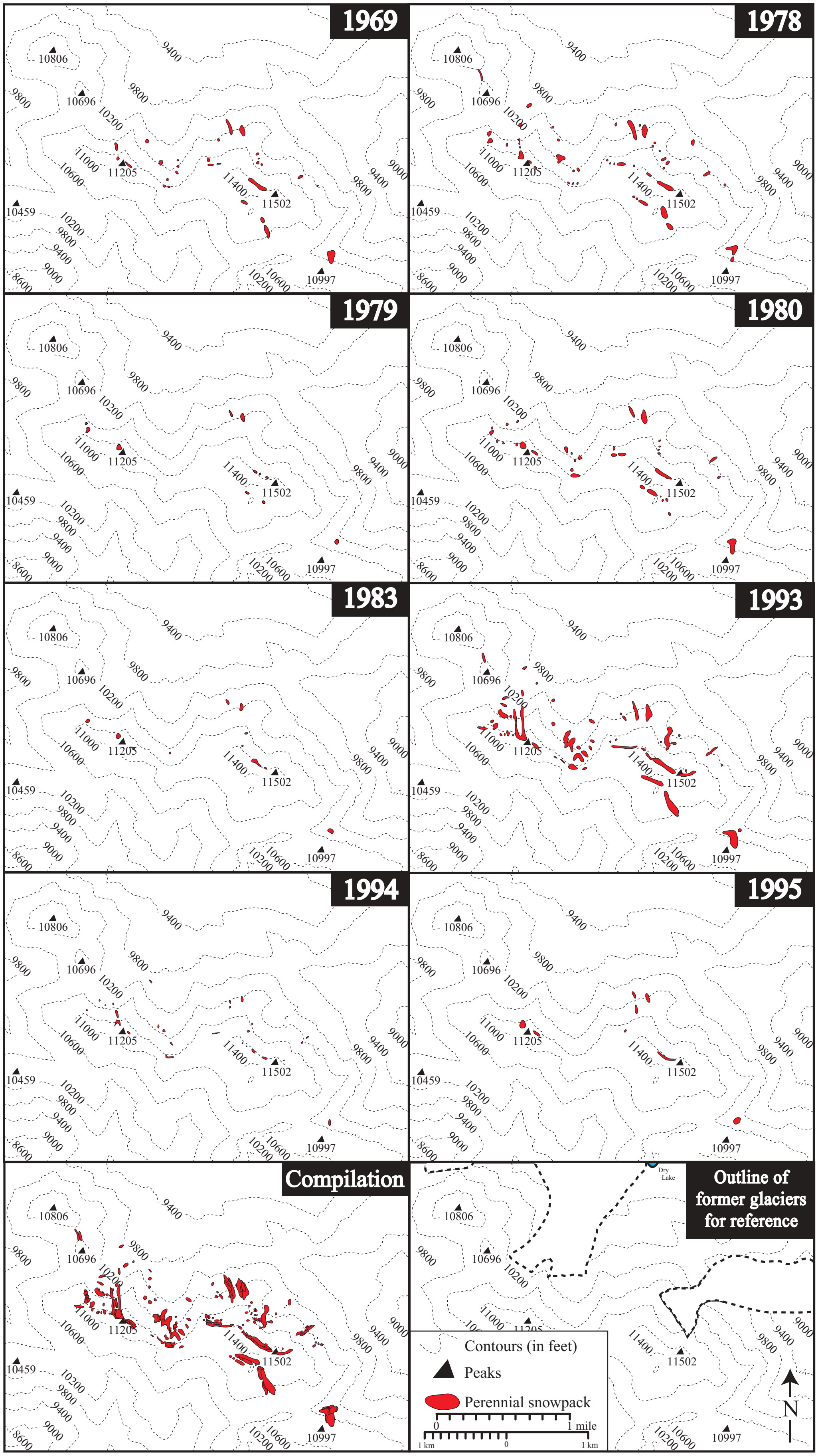

Figure DR1. Perennial snow patches on San Gorgonio Mountain for years during the period between 1969-1995, with compilation showing the main areas where snow persists.

Appendix 1: Cosmogenic radionuclide ^{10}Be dating methods and results

All the rocks sampled were monzogranites and gneisses. We sampled ~500 g of rock from the most horizontal surface on the top of each boulder by chiseling off the outer 1–5 cm. The latitude, longitude, and altitude of each sample were determined using a handheld global positioning unit, and topographic shielding was determined by measuring the skyline from each boulder using an inclinometer and compass. A description of the local setting and the characteristics of each boulder were recorded and photographs were taken.

Of each sample ~500 g was crushed and sieved to separate out the 250–500 μm size fraction for further analysis. Clean quartz was isolated from each sample using HCl and HF:HNO_3 leaching (Kohl and Nishiizumi, 1992) and a Frantz magnetic separator. Beryllium carrier was then added and the quartz was dissolved in HF/HNO_3. After dissolution the sample was fumed to dryness three times with perchloric acid to remove fluoride. The samples were run through anion and cation exchange resins to collect the Be fraction. Individual samples next were dried and then ignited to produce BeO. The BeO was crushed with Nb powder and then loaded into aluminum cathodes for measurement with the accelerator mass spectrometer (AMS). The AMS measurements for the ^{10}Be were carried out at the Lawrence Livermore National Laboratory AMS facility (Davis et al., 1990). ^{10}Be measurements were normalized to an ICN standard prepared by K. Nishiizumi using a half-life of 1.5 x 10^6 yr.

The measured isotope ratios were converted to radionuclide concentrations in quartz using the total beryllium in the samples and the sample weights. Radionuclide concentrations were then converted to zero-erosion exposure ages using a sea-level high latitude (SLHL) ^{10}Be production rate of 5.2 at/g-quartz/yr. The beryllium production rate used is based on a number of independent measurements of production rate as discussed by Owen et al. (2001; 2002). Production rates were scaled to the latitude and elevation of the San Gorgonio sampling sites using the star scaling factors of Lal (1991) and an assumed 3% SLHL muon contribution to production rates, and were further corrected for changes in the geomagnetic field over time. Details of the calculation were given in Owen et al. (2001, 2002).

TABLE 1. SAMPLE NUMBERS, LOCATIONS, AND COSMOGENIC RADIONUCLIDE ^{10}Be DATA AND AGES FOR BOULDERS ON MORAINES ON SAN GORGONIO MOUNTAIN

Sample number	Latitude (±0.01°N)	Longitude (±0.01°W)	Altitude (m above sea level)	Shielding factor	^{10}Be (10^6 /g	atoms quartz)	Exposure (years)	age	Geomagnetic correction (years)	
SG1	34°06.996'N	116°49.961'W	2850	0.99	1012474	± 27091	13369 ±	358	14254 ±	381
SG2	34°07.045'N	116°49.917'W	2825	0.99	1120663	± 29938	15113 ±	404	16085 ±	430
SG3	34°07.067'N	116°49.879'W	2824	0.99	1134244	± 38667	15212 ±	519	16190 ±	552
SG4	34°07.077'N	116°49.834'W	2825	0.99	1113386	± 29041	14923 ±	389	15888 ±	414
SG5	34°07.097'N	116°49.819'W	2816	0.99	1174714	± 30854	15834 ±	416	16836 ±	442
SG6	34°07.246'N	116°49.815'W	2800	0.99	1079593	± 28622	14691 ±	390	15645 ±	415
SG7	34°07.251'N	116°49.828'W	2797	0.99	503007	± 12960	14926 ±	385	15891 ±	409
SG8	34°07.263'N	116°49.854'W	2804	0.99	516507	± 14172	15263 ±	419	16241 ±	446
SG9	34°07.269'N	116°49.869'W	2798	0.99	497380	± 13536	14750 ±	401	15707 ±	428
SG10	34°07.274'N	116°49.877'W	2822	0.99	480765	± 18429	14048 ±	539	14973 ±	574
SG11	34°06.257'N	116°50.333'W	3142	0.99	75475	± 5212	1820 ±	126	2027 ±	140
SG12	34°06.254'N	116°50.330'W	3145	0.99	253542	± 11012	6109 ±	265	6685 ±	290
SG13	34°06.251'N	116°50.328'W	3149	0.99	135730	± 7091	3261 ±	170	3912 ±	204
SG14	34°06.259'N	116°50.324'W	3142	0.99	236411	± 7585	5706 ±	183	6314 ±	203
SG15	34°06.501'N	116°50.291'W	3037	0.99	503736	± 13151	12944 ±	338	13805 ±	360
SG16	34°06.536'N	116°50.269'W	3018	0.99	451488	± 11886	11730 ±	309	12486 ±	329
SG17	34°06.547'N	116°50.262'W	3016	0.99	476375	± 12673	12392 ±	330	13207 ±	351
SG18	34°06.555'N	116°50.262'W	3011	0.99	493580	± 13488	12880 ±	352	13734 ±	375
SG19	34°06.544'N	116°50.269'W	3019	0.99	324403	± 9465	8416 ±	246	8960 ±	261
SG20	34°07.291'N	116°51.474'W	2932	0.99	684650	± 17155	18742 ±	470	19860 ±	498
SG21	34°07.404'N	116°51.307'W	2886	0.99	440836	± 11728	12387 ±	330	13196 ±	351
SG22	34°07.423'N	116°51.193'W	2848	0.99	501659	± 13043	14430 ±	375	15375 ±	400
SG23	34°07.392'N	116°51.128'W	2964	0.99	480477	± 12583	12886 ±	338	13740 ±	360
SG24	34°07.386'N	116°51.109'W	2847	0.99	475828	± 11941	13693 ±	344	14602 ±	366
SG25	34°07.532'N	116°50.998'W	2764	0.99	619049	± 15446	18751 ±	468	19861 ±	496
SG26	34°07.530'N	116°50.983'W	2761	0.99	647705	± 15939	19659 ±	484	20800 ±	512
SG27	34°07.547'N	116°50.987'W	2758	0.99	617677	± 15429	18779 ±	469	19890 ±	497
SG28	34°07.536'N	116°50.970'W	2750	0.99	1019704	± 24378	31244 ±	747	32174 ±	769
SG29	34°06.289'N	116°49.387'W	3157	0.99	408038	± 10834	9772 ±	260	10343 ±	275
SG30	34°06.291'N	116°49.388'W	3160	0.99	499585	± 14190	11950 ±	339	12731 ±	362
SG31	34°06.307'N	116°49.421'W	3167	0.99	496404	± 12813	11819 ±	305	12590 ±	325
SG32	34°06.307'N	116°49.419'W	3166	0.99	439130	± 11580	10458 ±	276	11098 ±	293
SG33	34°06.299'N	116°49.156'W	3081	0.99	602483	± 17755	15102 ±	445	16086 ±	474
SG34	34°06.291'N	116°49.166'W	3076	0.99	890216	± 21729	22417 ±	547	23598 ±	576
SG35	34°06.321'N	116°49.159'W	3077	0.99	580793	± 14755	14582 ±	371	15545 ±	395
SG36	34°06.323'N	116°49.157'W	3079	0.99	582355	± 21375	14605 ±	536	15568 ±	571

SG37	34°06.355'N	116°48.723'W	2913	0.99	644138	± 16149	17840 ±	447	18922 ±	474
SG38	34°06.355'N	116°48.736'W	2916	0.99	503209	± 13011	13899 ±	359	14822 ±	383
SG39	34°06.394'N	116°48.688'W	2915	0.99	679130	± 16894	18791 ±	467	19909 ±	495
SG40A	34°06.415'N	116°48.703'W	2923	0.99	574972	± 14621	15822 ±	402	16828 ±	428
SG40B	34°06.415'N	116°48.703'W	2923	0.99	547307	± 13942	15058 ±	384	16033 ±	408
SG41	34°06.462'N	116°50.824'W	3123	0.99	398245	± 13581	10129 ±	345	10734 ±	366
SG42	34°06.462'N	116°50.829'W	3126	0.99	335301	± 11213	8723 ±	292	9289 ±	311
SG43	34°06.455'N	116°50.816'W	3128	0.99	313451	± 11278	7976 ±	287	8484 ±	305
SG44	34°06.465'N	116°50.832'W	3121	0.99	292923	± 10497	7450 ±	267	7920 ±	284
SG45	34°06.508'N	116°50.815'W	3098	0.99	445983	± 14354	11581 ±	373	12327 ±	397
SG46	34°06.505'N	116°50.817'W	3093	0.99	358531	± 12160	9206 ±	312	9744 ±	331
SG47	34°06.508'N	116°50.822'W	3093	0.99	180856	± 10522	4714 ±	274	5400 ±	314
SG48	34°06.582'N	116°50.714'W	3048	0.99	494655	± 28256	13056 ±	746	13926 ±	796
SG49	34°06.575'N	116°50.707'W	3049	0.99	440894	± 13387	11604 ±	352	12350 ±	375
SG50	34°06.577'N	116°50.688'W	3045	0.99	470939	± 14409	12402 ±	380	13218 ±	404

ADDITIONAL REFERENCES CITED

Davis, J.C., Proctor, I.D., Southon, J.R., Caffee, M.W., Heikkinen, D.W., Roberts, M.L., Turteltaub, K.W., Nelson, D.E., Loyd, D.H. and Vogel, J.S., 1990, LLNL/UC AMS facility and research program: Nuclear Instruments and Methods in Physics Research, v. B52, p. 269–272.

Kohl, C.P., and Nishiizumi, K., 1992, Chemical isolation of quartz for measurement of in-situ-produced cosmogenic nuclides: Geochimica et Cosmochimica Acta, v. 56, p.3583–3587.

Lal, D., 1991, Cosmic ray labeling of erosion surfaces: In situ nuclide production rates and erosion models: Earth and Planetary Science Letters, v. 104, p. 429–439.

Owen, L.A., Gualtieri, L., Finkel, R.C., Caffee, M.W., Benn, D.I., and Sharma, M.C., 2001, Cosmogenic radionuclide dating of glacial landforms in the Lahul Himalaya, Northern India: Defining the timing of late Quaternary glaciation: Journal of Quaternary Science, v. 16, p. 555–563.

Owen, L.A., Finkel, R.C., Caffee, M.W., and Gualtieri, L., 2002, Timing of multiple glaciations during the late Quaternary in the Hunza Valley, Karakoram Mountains, northern Pakistan: Defined by cosmogenic radionuclide dating of moraines: Geological Society of America Bulletin, v. 114, p. 593–604.

Appendix 2: Equilibrium-line altitude reconstructions

Equilibrium-line altitudes (ELAs) were calculated using the maximum altitude of preserved lateral moraines within each glacial stage. Both the accumulation area ratio (AAR) and the toe-to-headwall altitude ratio (THAR) methods of Furbish and Andrews (1984) and Meierding (1982) were used. We applied an AAR of 5.0–8.0 that is typical of mountain glaciers (Benn and Gemmell, 1997) and a THAR of 0.7 as used by Clark et al (1994) in the Sierra Nevada for debris-covered glaciers. This range of values helps take into account the influence of thick debris cover on these glaciers that may significantly reduce the size of the ablation zone.

Minnich (1984, 1986) showed that at 3200 m above sea level (asl) (700 mbar) the contemporary mean July temperature and precipitation on San Gorgonio Mountain is ~10 ^{o}C and 700-1000 mm yr^{-1}. The relation between precipitation and temperature at glacier ELAs derived by Ohmura et al. (1992) indicates that the temperature at a hypothetical contemporary San Gorgonio ELA should be between 0.5 and 1 ^{o}C. The average global environmental lapse rate of 6 ^{o}C km^{-1} implies that this temperature will occur at an altitude of 4700–4780 m asl in the San Gorgonio Mountains. During summer in California, however, environmental lapse rates are close to the dry adiabatic rate of 10 ^{o}C km^{-1} due to the existence of a strong sensible heat flux and the absence of latent fluxes. This lapse rate suggests that a hypothetical contemporary ELA would be at an altitude of between 4100 to 4150 m asl. Burbank (1991) showed that the ELAs for contemporary glaciers in the Sierra Nevada increased to the SSE by ~2.0 m km^{-1}, ranging from ~3500 m asl at Ritter Range (37.7^{o}N) to ~3800 m asl on Olancha Peak (36.3^{o}N). If this gradient is regionally consistent, the hypothetical contemporary ELA on San Gorgonio, ~270 km SSW of Olancha Peak, should be ~4340 m asl. Thus the ELA for a hypothetical contemporary glacier on San Gorgonio Mountain is in the range of 4100–4780 m asl.

On the basis of packrat midden data, Van Devender (1990) and Spaulding (1990) suggested that during the LGM, precipitation in the Sonoran and Mojave Deserts was 50% and <40% higher than today. The high-pressure system produced by the Laurentide ice sheet steered the mid-latitude jet stream to the south, leading to an increased vapor flux on San Gorgonio Mountain. It is likely that precipitation there during glacial times was at least 50% higher than today and hence was probably between 1000 and 2000 $mmyr^{-1}$. The precipitation-temperature relationships of Ohmura et al. (1992) suggest that the temperature at the ELA during glacial times was probably between 1 and 4 ^{o}C as the result of this increase in precipitation. We therefore used the reconstructed ELAs to calculate a range of ELA depressions and mean July temperature differences based on environmental lapse rates ranging between 6 and10 $^{o}C/km$ and the reconstructed ELAs for each glacial advance: 1200–1980 m (8.3–13.8 ^{o}C), 955–1925 m (6.6–13.3 ^{o}C), 900–1710 m (6.0–11.1 ^{o}C) and 950–1660 m (6.5–10.6 ^{o}C) for stages I, II, III and V, respectively.

REFERENCES CITED

Benn, D.I., and Gemmell, A.M.D., 1997, Calculating equilibrium-line altitudes of former glaciers by the balance ratio method: A new computer spreadsheet: Glacial Geology and Geomorphology: http://ggg.qub.ac.uk/ggg/papers/full/1997/tn011997/tn01.html.

Burbank, D.W., 1991, Late Quaternary snowline reconstructions for the southern and central Sierra Nevada, California and a reassessment of the “Recess Peak Glaciation”: Quaternary Research, v. 36, p. 294–306.

Clark, D.H., Clark, M.M., and Gillespie, A.R., 1994, Debris-covered glaciers in the Sierra Nevada, California, and their implications for snowline reconstructions: Quaternary Research, v. 41, p. 139–153.

Furbish, D.J., and Andrews, J.T., 1984, The use of hypsometry to indicate long-term stability and response of valley glaciers to changes in mass transfer: Journal of Glaciology, v. 30, p. 199–211.

Meierding, T.C., 1982, Late Pleistocene glacial equilibrium-line in the Colorado Front Range: A comparison of methods: Quaternary Research, v. 18, p. 289–310.

Minnich, R.A., 1984, Snow drifting and timberline dynamics on Mount San Gorgonio, California, USA: Arctic and Alpine Research, v. 16, p. 395-412.

Minnich, R. A., 1986, Snow levels and amounts in the mountains of southern California: Journal of Hydrology, v. 86, p. 37-58.

Ohmura, A., Kasser, P., and Funk, M., 1992, Climate at the equilibrium line of glaciers: Journal of Glaciology, v. 15, p. 403–415.

Spaulding, W.G., 1990, Vegetational and climatic development of the Mojave Desert: the last Glacial Maximum to the Present, *in* Betancourt, J.L., et al., eds., Packrat middens: The last 40,000 years of biotic change: Tucson, University of Arizona Press, p. 166–199.

Van Devender, T.R., 1990, Late Quaternary vegetation and climate of the Chihuahuan Desert, United States and Mexico, *in* Betancourt, J.L., et al, eds., Packrat Middens: The last 40,000 years of biotic change: Tucson, University of Arizona Press, p. 134–165.

TABLE 2. ELA CALCULATIONS USING THE HEIGHT OF THE HIGHEST LATERAL MORAINE, AN ACCUMULATION AREA RATIO OF 0.5 AND 0.8 (IN BOLD) A TOE-TO-HEAD ALTITUDE RATIO OF 0.7 (IN ITALICS*) AND ESTIMATES OF LOWERING OF MEAN JULY TEMPERATURES DURING EACH GLACIAL ADVANCE

Stage	Dollar lake (m)	Dry lake (m)	North Fork (m)	æELA (m) using a lapse rate of 6° C/km	æELA (m) using a lapse rate of 10° C/km	æ Mean July temperature (°C) using a lapse rate of 6° C/km	æ Mean July temperature (°C) using a lapse rate of 10° C/km	Range of æ Mean July temper-ature (°C)
I	2900 **2720–2800** *>2750*	----	2850 **2795–2900** *>2920*	1980–1880	1200–1430	8.3–11.4	9.0–13.8	8.3–13.8
II	2970 **2810–2835** *>2860*	2970 **2775–2900** *>2790*	3145 **2890–2950** *>2980*	1925–1635	955–1375	6.8–11.1	6.6–13.3	6.6–13.3
III	3140	3000 **2990–3055** *>2990*	3170 **3140–3200** *>3240*	1710–1580	900–1160	6.5–9.8	6.0–11.1	6.0–11.1
IV	----	Big Draw 3150 **3040–3140** *>3020* Little Draw 3130 **3030–3080** *>3030*	----	1660–1630	950–1110	6.8–9.5	6.5–10.6	6.5–10.6

Notes: * Minimum values of THAR (Meierding, 1982) are quoted because of the uncertainty of defining the highest glacial limits